Fracture Mechanics of Concrete and Concrete Structures -
High Performance, Fiber Reinforced Concrete, Special Loadings and Structural Applications- B. H. Oh, et al. (eds)
 ISBN 978-89-5708-182-2

Effect of aggregates morphology on the THM behaviour of concrete at high temperatures

T.T.H. Le & H. Boussa
Université Paris-Est, France

F. Meftah
Université Cergy-Pontoise, France

ABSTRACT: The aim of this contribution is to proceed to the numerical modelling of the thermo-hygro-mechanical behaviour of concrete by starting at the mesoscale level: the scale at which coarse aggregates are embedded in a mortar matrix (hardened cement paste and fine aggregates). The objective is then to identify the influence of the morphology and the aggregates distribution on the concrete behaviour at high temperatures. For this purpose, different bidimensional configurations of representative elementary volumes (REV) of concrete are investigated using both real and idealized finite element meshed aggregates geometries. Then numerical simulations are performed and results are discussed in terms of the heterogeneity effect on temperature, pressures and damage field profiles.

1 INTRODUCTION

Concrete is a widely used material in Civil Engineering (Building, Tunnel ...). In the recent years, there were often fires in tunnels and buildings which cause very serious consequences in terms of human and economic losses. When concrete is subjected to a high temperature, the material is the seat of numerous degradation processes. Among them, the aggregate-paste incompatibility may have a direct influence on the material stability: a deterioration of the mechanical properties of the material and its spalling in summary. Indeed, the thermal expansion of aggregates contrasts with the drying and dehydration induced shrinkage that arises in the cement paste due to physical and chemical transformations when temperature increases. Therefore, self equilibrated tensile stresses arise in the material which generate micro-cracking in the bulk of the cement matrix and at the matrix-granular inclusion interface. The assessment of this degradation process requires developing full coupled thermo-hygro-mechanical modeling approaches at the scale of occurrence of these degradation processes. However, the THM behaviour of concrete was mainly investigated at the macroscopic scale, at which concrete is regarded as a homogeneous material (Alnajim 2004, Gawin et al. 2003, Obeid et al. 2001), which partially precludes the effects of the microstructure on the overall THM behaviour. On the other hand, the thermo-mechanical mesocopic modelling of behaviour of damaged concrete has been studied on two dimensional configurations and where aggregates morphology has been idealized (Grondin et al. 2007). In particular, the effect of the aggregates nature, morphology and distribution on the propagation and percolation of the rising micro-cracks induced by the incompatibility between the cement matrix and of the granular inclusions needs further investigations. This issue is of a prime importance in order to assess the role that the microstructure may have in the material spalling: granular distribution and morphology may lead to preferential percolation paths of micro-cracking which may in turn control the flak geometry.

In this contribution, a finite element THM modelling of concrete at the meso-scale level is presented. Bi-dimensional finite element configurations of representative elementary volumes (REV) are generated by distinguishing the cement paste form the aggregates with different considered morphologies, size distributions. The THM approach is developed within the framework of partially saturated media. It allows describing the major mechanisms of mass transport, heat transfer, phase change (vaporization and dehydration) and their interaction with the mechanical behaviour of the different constituents.

Numerical simulations are then performed in order to carry out the influence of the aggregates nature, morphology and distribution on the behaviour of concrete at high temperatures.

2 MULTI-SCALE MODELLING

The purpose is to proceed to the simulation of the THM behaviour of a concrete by starting at the mesoscale: the scale at which coarse aggregates are embedded in a mortar matrix (hardened cement paste and fine aggregates).

The inclusions (coarse aggregates) may be seen either as hygrally inert or behaving as a partially saturated medium. In this analysis, studied aggregates are considered to have a weak connect porous network and a low initial saturation. Their hygral behaviour is then marginal and a thermal model is sufficient to describe their behaviour within the concrete mix. Therefore, only the mortar matrix is considered to have a full thermo-hygral behaviour with an ad hoc model.

Concerning the mechanical behaviour, the aggregates are considered (as a first approach) to be thermo-elastic while a Mazars's damage model (Mazars 1984) is adopted for mortar.

2.1 *Thermo-hygral model*

2.1.1 *Mortar*

The thermo-hygral model for mortar starts from a set of microscopic balance equations of mass and energy of each constituent of the medium: solid skeleton, liquid water, vapour water and dry gas. The approach is based on a space averaging theory proposed by Schrefler and co-workers (Gawin et al. 2003), (Lewis & Schrefler 1998). It allows describing the major mechanisms of mass transport, heat transfer, phase change (vaporisation and dehydration). The governing equations of the model are given in terms of the chosen state of variables. In this approach, they are the dry air pressure p_a, the water vapour pressure p_v and the absolute temperature T.

The mass balance equations of the constituent can put in the following generic form:

$$\frac{\partial m_\pi}{\partial t} + \nabla \cdot \left(m_\pi \boldsymbol{v}_{\pi-s} \right) = \dot{m}_\pi^r \tag{1}$$

where t = stands for time; m_π = mass per unit volume of each constituent ($\pi = s$ for solid, l for liquid, v for vapour and a for dry air); $\dot{m}_\pi^r$ = source term; and $\boldsymbol{v}_{\pi-s}$ = velocity of each constituent with respect to the solid phase. The mass m_π of each constituent is given by:

$$m_s = (1-\phi)\rho_s \;\; ; \quad m_l = \rho_l S_l \phi \;\; ; \quad m_v = \rho_v (1-S_l)\phi \;\; ; \quad m_a = \rho_a (1-S_l)\phi \tag{2}$$

where ρ_π = corresponding density; ϕ = porosity; and S_l = liquid saturation degree. The source term $\dot{m}_\pi^r$ is given by:

$$\dot{m}_s^r = \dot{m}_{dehyd} \;\; ; \quad \dot{m}_l^r = -\dot{m}_{vap} - \dot{m}_{dehyd} \;\; ; \quad \dot{m}_v^r = \dot{m}_{vap} \;\; ; \quad \dot{m}_a^r = 0 \tag{3}$$

where $\dot{m}_{vap}$ = rate of mass due evaporation / condensation phase change; and $\dot{m}_{dehyd}$ = rate of mass due to dehydration.

The mass transport of each constituent within the porous network is given by Darcy's law (for permeation) and Flick's law (for diffusion). Therefore, the mass fluxes write:

$$m_l \boldsymbol{v}_{l-s} = -K \frac{\rho_l k_{rl}}{\mu_l} \nabla p_l \tag{4}$$

$$m_v \boldsymbol{v}_{v-s} = m_v \boldsymbol{v}_{g-s} + m_v \boldsymbol{v}_{v-g} = -K \frac{\rho_v k_{rg}}{\mu_g} \nabla p_g - D\rho_g \frac{M_v M_a}{M_g^2} \nabla \left(\frac{p_v}{p_g} \right) \tag{5}$$

$$m_a \boldsymbol{v}_{a-s} = m_a \boldsymbol{v}_{g-s} + m_a \boldsymbol{v}_{a-g} = -K \frac{\rho_a k_{rg}}{\mu_g} \nabla p_g - D\rho_g \frac{M_v M_a}{M_g^2} \nabla \left(\frac{p_a}{p_g} \right) \tag{6}$$

where $\boldsymbol{v}_{g-s}$ = velocity of the gas mixture with respect to the solid phase; $\boldsymbol{v}_{v-g}$ and $\boldsymbol{v}_{a-g}$ = velocity of the vapour and dry air with respect to the gas mixture; $p_g = p_v + p_a$ = pressure of gas phase; p_l = pressure of liquid water; K = intrinsic permeability; $k_{r\pi}$= relative permeability of π phase ($\pi = g$ for gas and $\pi = l$ for liquid); μ_π = dynamic viscosity; D = effective diffusivity; and M_v, M_a and M_g = molar mass of vapour, dry air and gas phase, considered as ideal gases.

Furthermore, the energy balance equation of the whole medium reads:

$$\sum_{\pi=s,l,v,a} \left(m_\pi C_\pi \right) \frac{\partial T}{\partial t} + \sum_{\pi=g,l} \left(m_\pi C_\pi \boldsymbol{v}_{\pi-s} \right) \cdot \nabla T + \nabla \cdot \boldsymbol{q} = -H_{vap} \dot{m}_{vap} + H_{dehyd} \dot{m}_{dehyd} \tag{7}$$

where C_π = heat capacity; $\boldsymbol{q}$ = heat flux given by Fourier's law; H_{vap} = enthalpy of vaporization; and H_{dehy} = enthalpy of dehydration.

The finite element model is derived starting from the weak forms of the set of the previous balance equations. By introducing the space discretization together with theta-method time discretization we have a schema at two levels of iterations. For more details of the finite element model, you can see in (Le et al. 2009, Meftah et al. 2009).

This TH model has been implemented in a finite element code Cast3M developed by the French research centre for nuclear energy (CEA). The model has been validated at the macroscopic scale (Le et al. 2009).

2.1.2 *Aggregates*

A pure thermal model is used for the simulation of aggregates behaviour within the concrete mix. This model starts from the classical linearized balance equation of heat:

$$\rho C_p \frac{\partial T}{\partial t} + \nabla \cdot \boldsymbol{q} = 0 \tag{8}$$

where ρ = density of the medium; C_p = specific heat; and $\boldsymbol{q}$ = heat flux given by Fourier's law.

Furthermore, an ideal interface is assumed between the aggregates and matrix. Therefore, no jump in the temperature field can be captured when crossing the interface. This aspect needs to be improved since water transport in the mortar phase can lead to strong temperature gradients close to the aggregates.

2.2 *Mechanical model*

An isotropic elastic-damage model (Mazars, 1984) is adopted here for the behaviour of mortar at high temperature. In summary, the stress tensor $\boldsymbol{\sigma}$ is given by:

$$\boldsymbol{\sigma} = (1-\omega)\boldsymbol{E} : \boldsymbol{\varepsilon}_e \tag{9}$$

where $\boldsymbol{\varepsilon}_e = \boldsymbol{\varepsilon} - \boldsymbol{\varepsilon}_\theta - \boldsymbol{\varepsilon}_{cr} - \boldsymbol{\varepsilon}_{sh} - ...$ is the elastic strain tensor obtained from the total one $\boldsymbol{\varepsilon}$ by removing free thermal expansion $\boldsymbol{\varepsilon}_\theta$, shrinkage $\boldsymbol{\varepsilon}_{sh}$, creep $\boldsymbol{\varepsilon}_{cr}$, etc… In this analysis, only thermal expansion is considered. Moreover, the evolution of damage ω is related to extension strains given by the positive part of the strain components. Note that no pressure effect is yet taken into account.

3 MESOSCALE NUMERICAL SIMULATIONS

3.1 *Studied configuration*

To study the effect of the microstructure on the deterioration of the material, $100 \times 100 \times 300$ mm^3 specimens of an ordinary concrete mix, with silico-calcareous (SC) aggregates and a w/c ratio of 0.54 (M40SC), are cut into several slices. Figure 1 gives face views of three investigated slices. The maximum aggregate size does not exceed 2.5cm which confers to the slices the feature of being representative element volumes. For each slice, the surface concentration of coarse aggregates (with a representative in-plan size greater than 3mm) is determined, the complementary part being the concentration of the homogeneous mortar matrix. The average (statistic) volume fraction of mortar is about 58% and therefore is 42% for coarse aggregates.

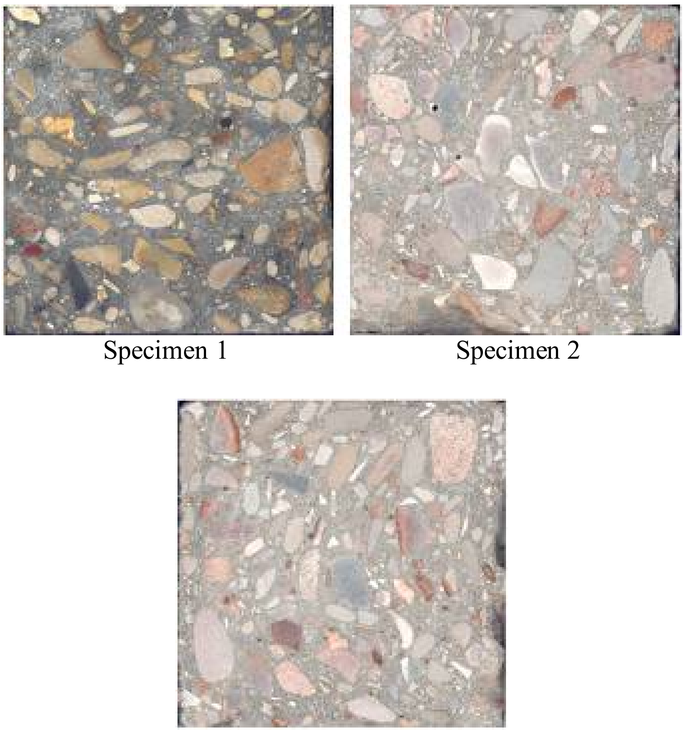
Specimen 1 Specimen 2

Specimen 3

Figure 1. Three scanned images of concrete.

The major thermal, hygral and mechanical properties of M40SC concrete are obtained experimentally from Mindeguia (2009). Concerning the individual components (mortar and SC aggregates), only some properties are available in the literature for the associated concrete mix (Menou 2004, Gaweska Hager 2004). Therefore, the missing parameters are estimated, when possible, by an inverse analysis using Mori-Tanaka's homogenization scheme (Benveniste 1986).

In order to perform two-dimensional simulations, the concrete slices (Fig. 1) have been used to generate finite element meshes of the two phases: coarse aggregates and mortar matrix.

For each specimen tow meshes are generated, one representing the real aggregates morphology with the other one is an ideal circular idealisation of these aggregates (Figs. 2-4). The ideal aggregates have the same barycentres and areas as the corresponding real ones.

In the numerical simulations, the specimens are heated at all faces by imposing a continuously increasing temperature by 1°C/min up to 250°C which is above the onset temperature of dehydration process in the cement paste. The surrounding external relative humidity is $h_r^{ext} = 50\%$ and convective mass boundary conditions are considered between the surface of the specimens and the surrounding medium.

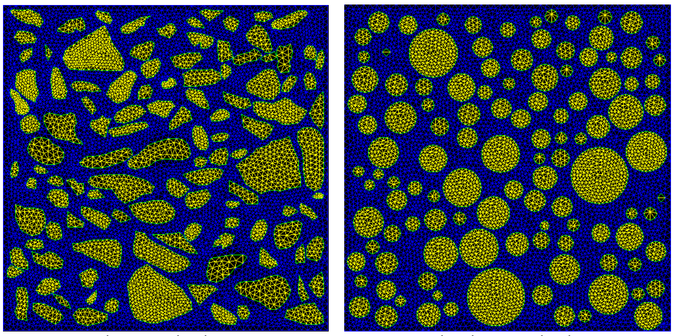

Figure 2. Meshes of real and idealized specimen 1.

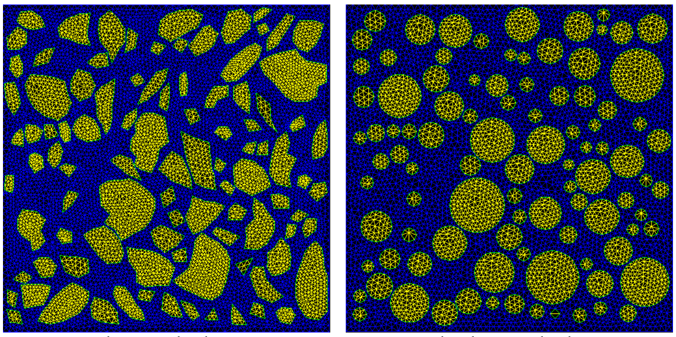

Figure 3. Meshes of real and idealized specimen 2.

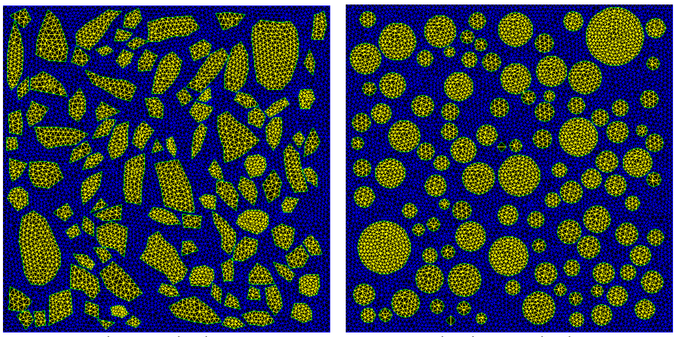

Figure 4. Meshes of real and idealized specimen 3.

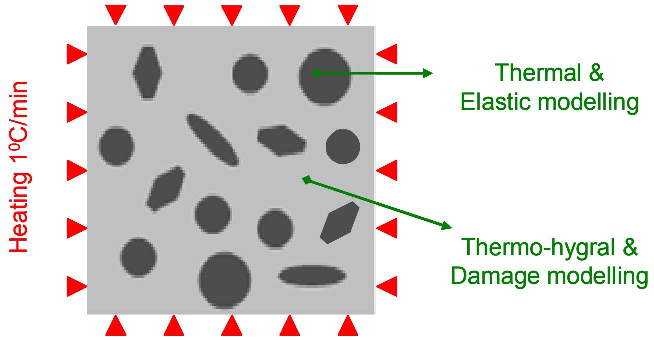

Figure 5. Loading and modelling.

3.2 *Thermo-hygral results*

Some first results are presented here in terms of thermo-hygral fields and damage profiles within the studied specimens.

The overall response of the different REV is given in by carrying out the simulated mass-losses and ratios of the temperature in the centre of the specimens to the temperature at their external heated surfaces. The temperature at the centre is obtained by averaging on a disc large enough to be representative of a mix of aggregates an matrix.

3.2.1 *Mass loss*

Figure 6 shows results of mass loss of the three studied concrete specimens either with a real morphology of aggregates or ideal one. There is no significant difference between simulated mass losses of these specimens. Even they are not yet fully dried up to 250°C (not yet stabilized mass-loss), the morphology and distribution of aggregates seems to have no significant effect on the global mass-loss of these concrete specimens. Thus, an ideal representation of aggregates appears to be acceptable for this purpose.

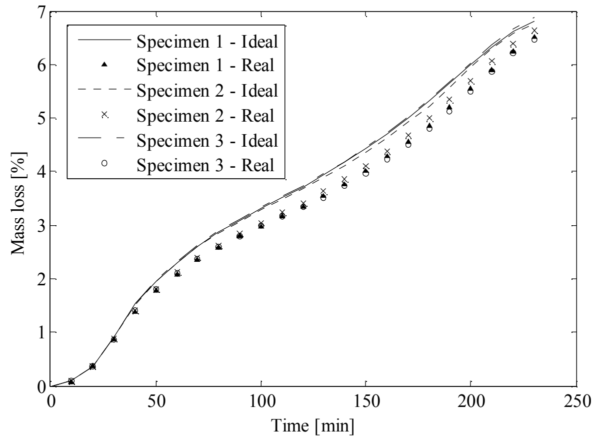

Figure 6. Mass loss.

3.2.2 *Temperature*

Time evolution of the temperature difference between the heated face and each specimen centre is presented on Figure 7. Similar results are obtained for the different specimens: a continuous increase up to a peak of almost 24°C at 220 minutes of heating. At this moment, the temperature at the face is equal to 240°C while its value at the centre is equal to 216°C. After the peak, a sharp decrease of the temperature difference is monitored. The moderate peak amplitude is mainly due to low heating rate adopted

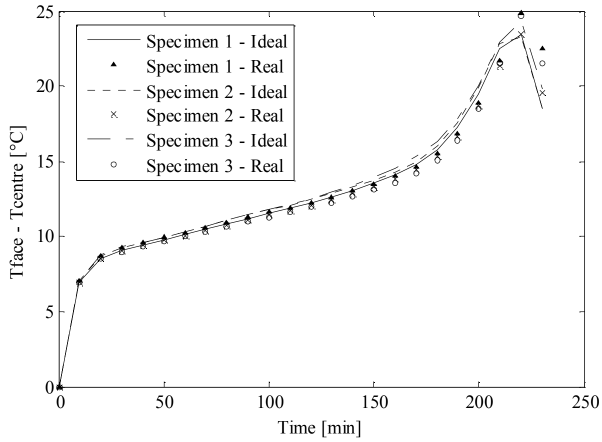

Figure 7. Evolution of heated face to specimen centre temperature difference.

here, that is, 1°C/min. It is worth noting that similar trends are obtained with a macroscopic approach (Kanema et al. 2007) in which it is shown that the peak amplitude of temperature difference between surface and specimen centre are controlled by initial water content of the cement paste.

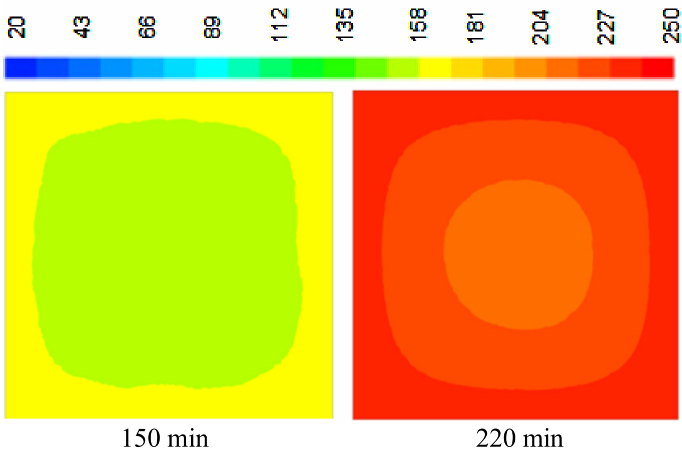

Figure 8. Iso-values of the temperature of real specimen 1 at 150 min and 220 min of heating.

With regard now to the temperature distribution within the specimen, Figure 8 presents the iso-values of the temperature of specimen 1 with real morphology at 150 min and 220 min of heating (this latter stage corresponds to the maximum temperature difference). For the different specimens, the temperature distribution is almost homogeneous at all time stages. Therefore, the distribution and the morphology of aggregates may have no effect on temperature profiles which would suggests that a macroscopic analysis or a mesoscale one with idealized representation of aggregates are acceptable to predict the thermal behaviour.

Nevertheless, this result has to be further analyzed in terms of either thermal conductivity contrast between constituents (aggregates and mortar matrix) or imperfect thermal interfaces between them.

3.2.3 *Gas pressure*

Here we discuss the effect of the distribution and the morphology of aggregates on the gas pressure in the mortar matrix only, since the aggregates are hygrally inert.

Figure 9 gives evolutions of the gas pressure at the centre of specimens with time.

The gas pressure increases and reaches a peak at about 220 minutes of heating, then, a decrease occurs. This result is common to all studied specimens regardless aggregate morphology: a slight discrepancy of less than 10% between the different configurations is obtained. Moreover, a comparison between Figure 7 and Figure 9 shows that the gas pressure peak occurrence coincides with the moment when the temperature difference, between the specimen heated surface and the material bulk, attains its maximum. This means that for the considered heating rate, thermal and hygral processes kinetics will lead simultaneously to maximum induced stresses in the specimen, that is, arising stresses due, respectively, to temperature gradients and to pore pressures. These are mechanisms generally admitted for heated concrete spalling (Gawin et al. 2005).

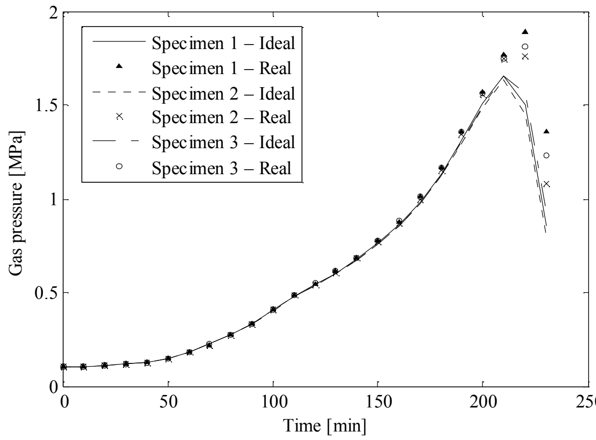

Figure 9. Gas pressures at the centre.

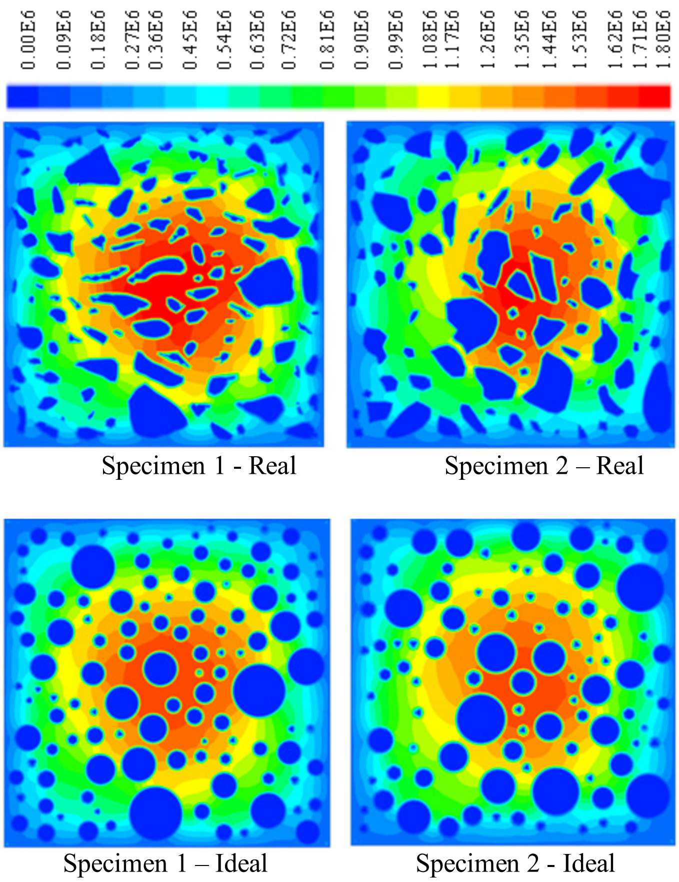

Figure 10. Iso-values of the gas pressure of specimen 1 and 2 at peak pressure occurrence.

Moreover, gas pressure distributions within specimens show strong local effects due the heterogeneity. An overpressure front propagates from specimen cover to the material bulk with a profile that locally depends on aggregates distribution and morphology as shown by gas pressure iso-values of Figure 10. Gas pressure induced tensile stresses which may lead to a microstructural effect (micro-cracking that arises when tensile stresses attain mortar matrix tensile strength which decreases with temperature), amplifying thus the structural effect generated by tensile stresses due to thermal expansion gradients at the macroscopic scale. Aggregates morphology and distribution will then control crack patterns, namely percolation paths as shown by damage profiles hereafter. Furthermore, gas pressure distribution also shows strong variations around large aggregates which may be expected to amplify local mechanical degradations at inclusion-matrix interfaces.

3.3 *Mechanical results*

Mechanical behaviour is analyzed in terms of damage profiles and deformation of specimens sketched in Figures 11-13 at time stages 150 min and 230 min (after that gas pressure peaks occur).

At the early stages (up to 150 min), it can be observed that damage occurs mainly at the mortar surrounding aggregates, that is, micro-cracks arise at the matrix-inclusion interfacial zone. Thereafter, the micro-cracks propagate across the mortar matrix following some preferential paths that clearly appear to be controlled by morphology of aggregates and their distribution. The bridging micro-cracks percolate to form some dominant macro-cracks that may emerge at the specimen surface.

The effect of morphology can be assessed by comparing damage profiles and crack patterns given by Figures 12 and 13 which concern specimens for which aggregates morphology is the only difference (real versus idealized) while the same distribution is

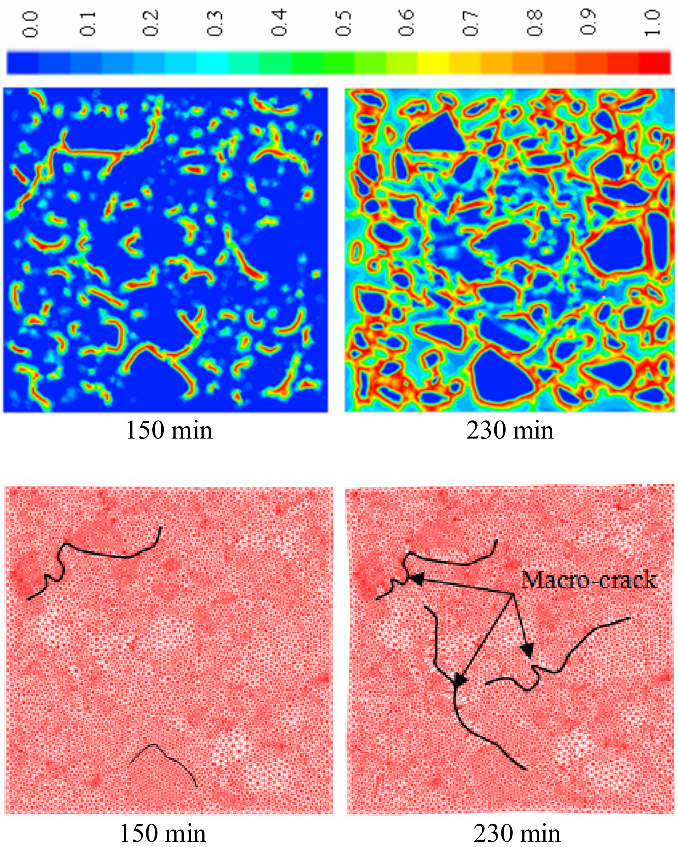

Figure 11. Specimen 1 – Real morphology: Damage profile (top), Deformed shape (bottom).

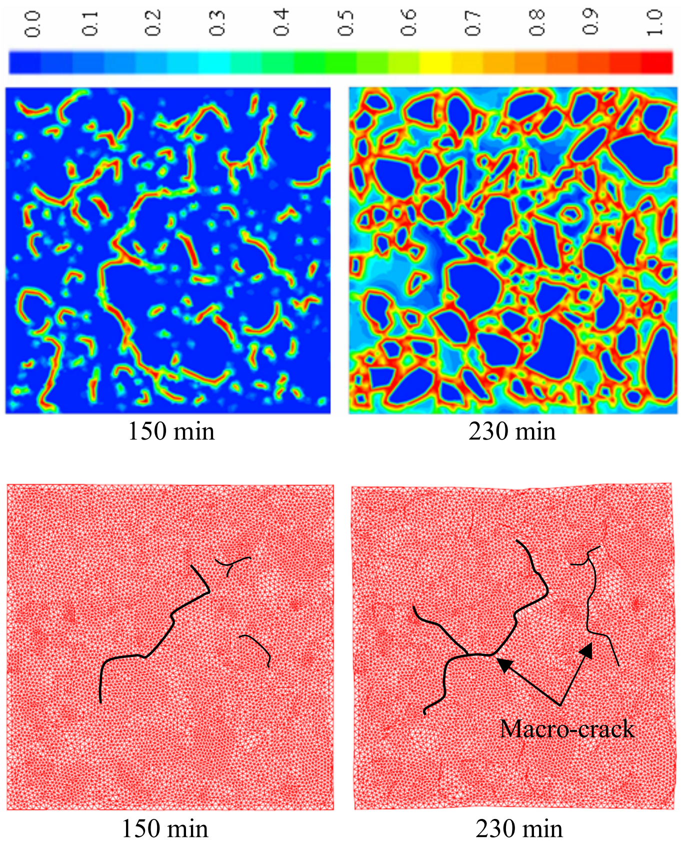

Figure 12. Specimen 2 – Real morphology: Damage profile (top), Deformed shape (bottom).

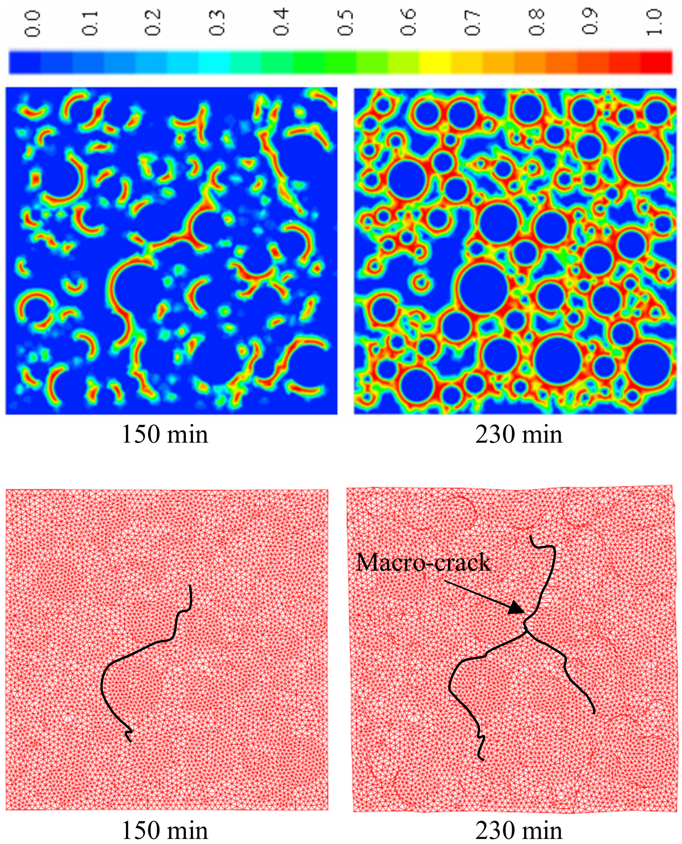

Figure 13. Specimen 2 – Ideal morphology: Damage profile (top), Deformed shape (bottom).

kept. Then, cracks propagate following different paths during heating, mainly at the final stages when localized macro-cracks form. Note that combined distribution and morphology effects are highlighted by comparing crack patterns of specimen 1 and specimen 2.

Similar behaviours had already been observed experimentally by Mindeguia (2009) and shown in Figure 14. Cracks network developing at the mortar-aggregates interface and then diffusing in the hole specimen can be visually observed.

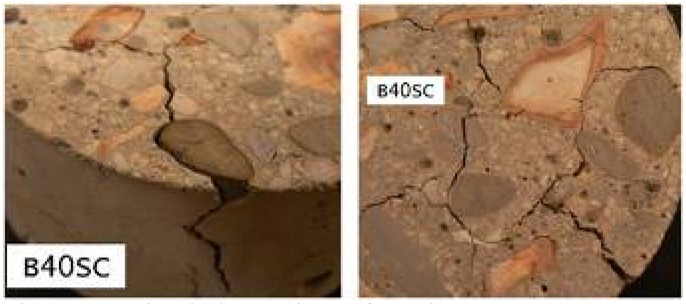

Figure 14. Visual observations of specimen B40SC at 400 °C (Mindeguia 2009).

In summary, the effect of the morphology and distribution of aggregates is not negligible on the stability of the concrete at high temperatures. This may be a reason to explain that during testing, with the same configuration, there are specimens that experience thermal instabilities while the others not (Mindeguia 2009).

4 CONCLUSION

An original thermo-hydro-mechanical (THM) modelling approach of concrete at the meso-scale level is presented and used to investigate the effects of aggregates morphology and distribution on the concrete behaviour during heating. The obtained results show that the heterogeneity does not affect neither the overall thermo-hygral behaviour of the material nor the local temperature evolution. By contrast, the local hygral behaviour and the mechanical degradation are strongly affected by the microstructure of the material.

Indeed, the hygral fields (gas pressure in this contribution, but also saturation) are strongly heterogeneous in the specimen. The distribution of the gas pressure in the mortar depends on the distribution and morphologies of aggregates: large aggregates prevent gas over pressure to dissipate when close to the external boundary.

With regard to the mechanical behaviour, the first results show that the damage occurs at the interface mortar / aggregates on all specimens and then develops into the mortar. This result is reasonable and similar with the experiment. The cracks appear first in the place where the aggregates are sufficiently close and then propagate into the mortar. Therefore, the effect of the morphology and distribution of aggregates is not negligible on the mechanical behaviour of the concrete at high temperatures.

These interesting new results are to be completed by extending the mechanical model in order to account for fluid pressure (gas and liquid when oversaturation occurs) effect at this scale, shrinkage and transient creep in the cement matrix. Furthermore, a 3D THM analysis is also under investigation. These are some perspectives to this work.

ACKNOWLEDGEMENTS

Numerical simulations are performed at Laboratoire de Modélisation et Simulation Multi Echelle (MSME) of Université Paris-Est Marne-la-Vallée, France. The authors are very grateful.

REFERENCES

Alnajim, A. 2004. Modélisation et simulation du comportement du béton sous hautes températures par une approche thermo-hygro-mécanique couplée. Application à des situations accidentelles. PhD thesis, Université de Marne-la-Vallée, France.

Benveniste, Y. 1986. On the effective thermal conductivity of multiphase composites. *Journal of Applied Mathematics and Physics* 37: 696-713.

Gaweska Hager, I. 2004. Comportement à haute température des bétons à haute performance - évolution des principales propriétés mécaniques. PhD thesis, Ecole Nationale des Ponts et Chaussées, France.

Gawin, D. & Pesavento, F. & Schrefler, B.A. 2003. Modelling of hygro-thermal behaviour of concrete at high temperature with thermo-chemical and mechanical material degradation. *Comput. Methods. Appl. Mech. Engrg* 192: 1731-1771.

Gawin, D. & Pesavento, F. & Schrefler, B.A. 2005. Towards prediction of the thermal spalling risk through a multi-phase porous media model of concrete. *Comput. Methods Appl. Mech. Engrg.*

Grondin, F. & Dumontet, H. & Ben Hamida, A. & Mounajed, G. & Boussa, H. 2007. Multi-scales modelling for the behaviour of damaged concrete. *Cement and Concrete Research* 37: 1453-1462.

Kanema, M. & De Morais, M.V.G. & Noumowe, A. & Gallias, J.-L. & Cabraillac R. 2007. Experimental and numerical studies of thermo-hydrous transfers in concrete exposo high temperature. *Heat and Mass Transfer* 44 (2).

Le, T.T.H. & Meftah, F. & Boussa, H. 2009. A multi-scale thermo-hydral modelling of concrte behaviour at high temperature. *Poro-Mechanics IV; Proceedings of the Fourth Biot Conference on Poromechanics, New York, 8-10 June 2009.* DEStech Publications, Inc.

Lewis, R.W. & Schrefler, B.A. 1998. *The Finite Element Method in the Static and Dynamic Deformation and Consolidation of Porous Media.* John Wiley & Sons.

Mazars, J. 1984. Application de la mécanique de l'endommagement au comportement non linéaire et à la rupture du béton de structure. PhD thesis, Université Paris 6, France.

Meftah, F. & Dal Pont, S. & Schrefler, B.A. 2009. A three-dimensional staggered finite element approach for modelling thermo-hygral coupled phenomena in porous media. *International Journal for Numerical and Analytical Methods in Geomechanics,* submitted.

Menou, A. & Mounajed, G. & Boussa, H. & Pineaud, A. & Carre, H. 2006. Residual fracture energy of cement paste, mortar and concrete subject to high temperature. *Theoretical and Applied Fracture Mechanics* 45.

Mindeguia, J.-C. 2009. Contribution expérimentale à la compréhension des risques d'instabilité thermique des bétons. PhD thesis, Université de Pau et des Pays de l'Adour, France.

Obeid, W. & Mounajed, G. & Alliche, A. 2001. Mathematical formulation of thermo-hygro-mechanical coupling problem in non saturated porous media. *Comput. Methods Appl. Mech. Engrg.* 190: 5105-5122.